JMEPEG (2010) 19:421–427
DOI: 10.1007/s11665-009-9508-5

1059-9495/$19.00

Tribological Properties of CrN/AlN Films Produced by Reactive Magnetron Sputtering

A. Rojo, J. Solís, J. Oseguera, O. Salas, and R. Reichelt

(Submitted October 30, 2008; in revised form June 12, 2009)

The microstructure of CrN/AlN films, prepared by reactive magnetron sputtering under various conditions, was analyzed and related to the wear behavior of the films. One set of films was prepared by conventional reactive magnetron sputtering, a second set adding an extra amount of reactive gas to the initial Ar + N_2 mixture and a third set adding an extra source of nitrogen near the substrate during sputtering. The samples were analyzed by scanning electron microscopy + energy dispersive microanalysis, high resolution scanning electron microscopy, atomic force microscopy, and x-ray diffraction. The results of the microstructural analysis revealed a clear difference in the morphology growth of the films when extra nitrogen was used compared to the conventionally prepared films. Formation of CrN was significantly faster than that of AlN. The most effective method to produce AlN was to introduce extra nitrogen. Pin-on-disk wear experiments were carried out in ambient air, to investigate the tribological behavior of the CrN/AlN system against a steel ball under dry conditions for various loads and a constant sliding speed. The results revealed that tribological properties of the layers improved unlike those of the untreated H13 steel. The friction behavior is closely related to the structure of the deposited films. The thicker CrN layer contributed to the higher load capacity of the coated steel when compared to the unmodified steel. However, wear life for the coating system was very short, denoted by the fairly poor adhesion of the film system to the steel substrate.

Keywords chromium nitride-aluminum nitride CrN/AlN, physical vapor deposition (PVD), reactive magnetron sputtering, tribological properties

1. Introduction

The tribological performance of hard multilayers is amply recognized (Ref 1, 2), in which the role of nitrides has been proven to be quite remarkable. In particular, single and multilayer films involving CrN have become the subject of many studies (Ref 3-10) and their excellent properties for specific types of applications have also been well established. On the other hand, AlN thin films have been widely investigated for electronic, acoustic, and optical applications (Ref 11-15), but their potential as tribological films has not been fully explored despite the remarkable mechanical properties of bulk AlN: Young′s modulus of 330 GPa and Knoop hardness of 10.8 GPa (Ref 16).

It is known that in order to take full advantage of these remarkable properties in coatings, not only does the structure of the nitrides have to be carefully tailored, but also the nitride layers should be combined with other materials to create a multilayer architecture that ensures the performance and integrity of the coating (Ref 1, 2). One of the most effective methods to generate this type of architecture is reactive magnetron sputtering. This method, not only allows the production of thin films with properties close to those obtained in the bulk, but also provides flexibility in terms of manipulating the processing conditions to change the structure of the films. Although studies on the tribological performance of systems that include the CrN/AlN layers have been put forth over the last few years (Ref 17-19), further research on the impact of the processing conditions is necessary. Since the coating-substrate interface, grain morphology, grain density, and the level of residual stresses depend on the deposition conditions, there is a need to explore the effect of different reactive atmospheres on the structure and tribological performance of the coatings.

In the present study, multilayered Cr/CrN/AlN coatings have been deposited by reactive magnetron sputtering on the surface of a H13 steel substrate, a material that is often used for tribological applications. The effect of the method of feeding the reactive gas during sputtering on the coating microstructure and its tribological performance were also investigated.

2. Experimental Procedure

2.1 Deposition Experiments

The multilayers were deposited by reactive magnetron sputtering in the chamber shown schematically in Fig. 1. The deposition system is composed of three planar nonbalanced magnetrons arranged in a vertical position each with a pure Al or pure Cr targets (50.8 mm in diameter). The substrate to

A. Rojo, ITESM-TOL, Eduardo Monroy Cárdenas 2000, Toluca 50110, Mexico; **J. Solís**, SEP-DGEST-ITTLA, Av. Mario Colín, S/N, Tlalnepantla Edo. de Méx 54070, Mexico; **J. Oseguera** and **O. Salas**, ITESM-CEM, Carretera a Lago de Guadalupe km 3.5, Atizapán 52926, Mexico; and **R. Reichelt**, Institut fuer Medizinische Physik und Biophysik, Westfaelische Wilhelms Universitaet, Robert-Koch-Str. 31, 48149 Muenster, Germany. Contact e-mail: josesolis@itesm.mx.

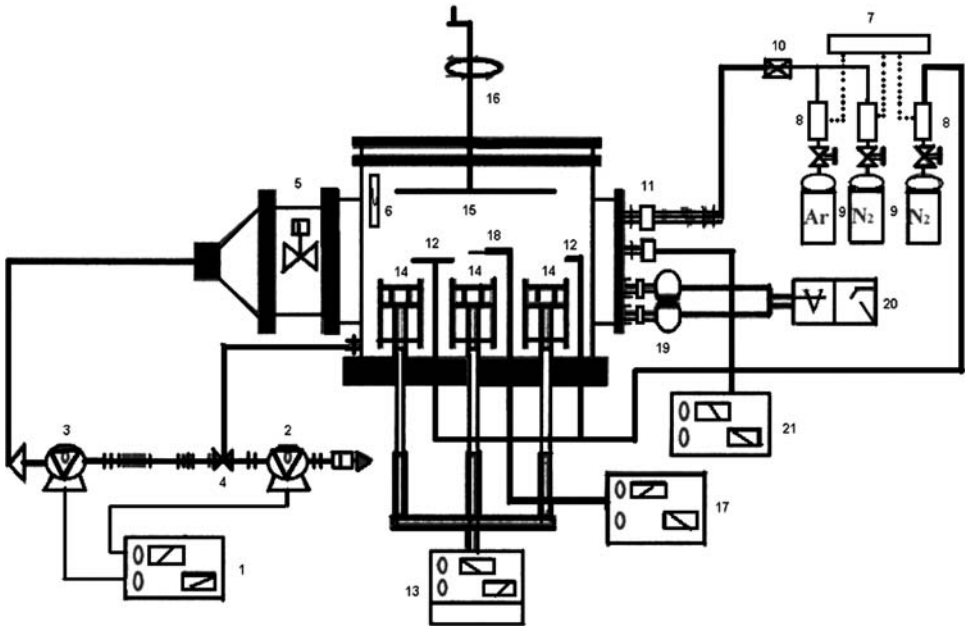

Fig. 1 Schematics of the experimental setup. Vacuum system (1-4). Valve to regulate conductance (5). Heating lamp (6). Flow controllers and mixed gases systems (7-11). Extra N_2 gas between target and substrate (12). Nonbalanced magnetrons and supply energy system (13 and 14). Sample holder (15). Chamber unit entrance (16). Langmuir probe and control (17 and 18). Pressure gauges (19 and 20). The OES (21)

Table 1 Relevant parameters for the deposition experiments

	Experiment		
	I	**B**	**B3**
Layers	CrN and AlN	CrN and AlN	CrN and AlN
Target	Cr and Al	Cr and Al	Cr and Al
Power for Cr target, W	50	50	50
Deposition time on Cr target, min	60	60	60
Extra gas of N_2 on Cr target	Yes	Yes	No
Direct gas of N_2 on Cr target	No	No	Yes
Voltage for Al target, V	450	450	250
Deposition time on Al target, min	30	30	30
Extra gas of N_2 on Al target	No	Yes	No
Direct gas of N_2 on Al target	No	No	Yes

target distance for Cr sputtering was an average of 31 mm ± 1 mm and for Al sputtering 29 mm ± 1.5 mm. The substrates were disks of 25.4 mm in diameter and 10 mm high cut from a H13 steel bar. Prior to the deposition experiments, the substrates were sanded with SiC papers, polished with 6 μm diamond paste to produce a mirror finish, and cleaned in an ultrasonic bath of ethanol for 3 min. The discharge was sustained by an Advance Energy DC power supply. Three different reactive atmospheres were explored in the present study: an Ar + N_2 mixture (experiment I), Ar + N_2 + extra N_2 injection between the target and the substrate as shown in

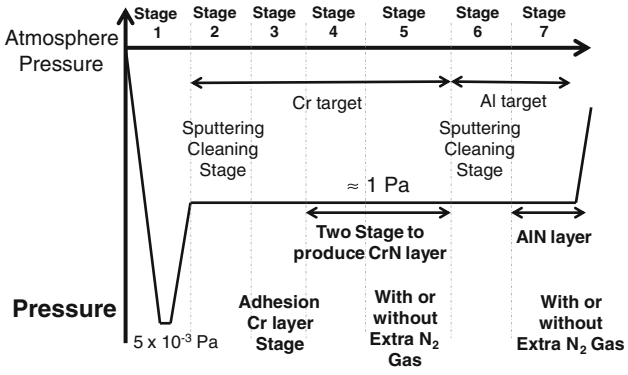

Fig. 2 Schematic description used to produce the CrN and AlN layers

Fig. 1 (Experiment B), and Ar + N_2 + direct N_2 injection near the substrate (Experiment B3). A summary of the deposition conditions for the three experiments is presented in Table 1.

Figure 2 describes a typical deposition sequence for the experiments. First, a Cr adhesion layer was sputtered with an Ar plasma, then the Ar + N_2 gas mixture was introduced during sputtering of the Cr target (when the extra N_2 injection was used, it was done during this step). Sputtering of the Al target followed, which was performed either with extra N_2, without extra N_2 or with direct N_2 insertion as with the Cr sputtering. For Al sputtering, voltage control was used while power control mode was selected for Cr sputtering.

Equipment for microstructural characterization of the deposited films included: a JEOL microscope model JSM6360LV used for scanning electron microscopy + energy dispersive microanalysis (SEM + EDS), a Bruker D8 (AXS) for x-ray Diffractometry (XRD), and an Autoprobe AP-100 for the atomic force microscopy (AFM).

2.2 Tribology Tests

2.2.1 Experimental Procedure. Dry wear resistance tests were performed. Tribological experiments were carried out using a real time pin-on-disk test machine from CSM instruments™, which continuously records friction coefficients as a function of time (see Fig. 3). A tribometry software package was used along with the tribometer for setting it up and handling the data. The experimental procedure was performed according to ASTM G99-95a (Ref 20). For the tribological tests, a 6-mm diameter AISI 52100 (100Cr6) steel ball rigidly held to the load arm was used as the pin static partner and the CrN/AlN bi-layer deposited on the H13 steel-base was employed as the disk. The following experimental parameters were kept constant for all tests: sliding velocity = 0.02 m s^{-1}; temperature 20 ± 3 °C; sliding distances 30-38 m, and the relative humidity 50 ± 5%, and a contact load of 1 N was vertically applied on the films.

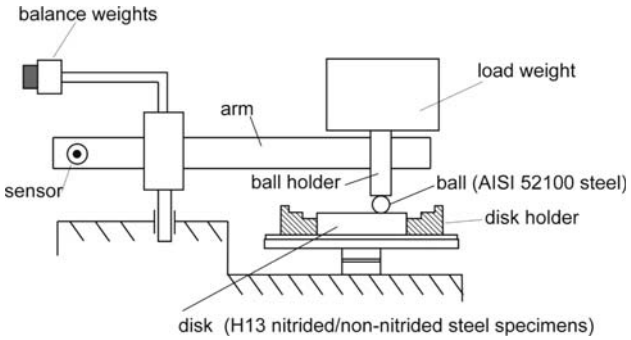

Fig. 3 Schematic diagram of the pin-on-disk wear test machine

3. Results and Discussion

3.1 Microstructural Characterization

Figure 4 shows the morphology of the films in cross-sectional and top SEM views of the three samples, while Fig. 5 depicts both a high resolution scanning electron microscopy (HRSEM) (a) and an AFM image (b) of sample B3. The cross-sectional views show that all the films developed a columnar structure and also display the thicknesses of the various films. The bottom layer, produced during reactive sputtering of the Cr target was always much thicker (around 10 times thicker) than that obtained during reactive sputtering of Al in all of the cases, more than that expected of twice the deposition time of Cr versus Al. There appears to be an effect of the processing conditions on the morphology of the films. The top micrographs, which correspond to the Al containing film, displayed nodular morphology, where individual nodules are likely to correspond to the top of the columns. The size of the top nodules which corresponds to the surface roughness decreased while the density of the columnar structure increased in each experiment (I $\rightarrow$ B $\rightarrow$ B3). This effect can be further analyzed in Fig. 5(b) which presents an AFM image of sample B3. Here, the top of the columns is better defined and their diameters can be measured on the order of tens of nanometers with a fairly homogeneous size distribution. A finer surface roughness may have a beneficial effect on the tribological behavior of the films.

The nature of the deposited layers was investigated by XRD and the results are shown in Fig. 6. According to the XRD results, formation of CrN was observed in all cases; however, production of AlN seems to have been more difficult, since its presence is only clear in sample B. Furthermore, it seems that adding extra nitrogen near the substrate (sample B3) was not as

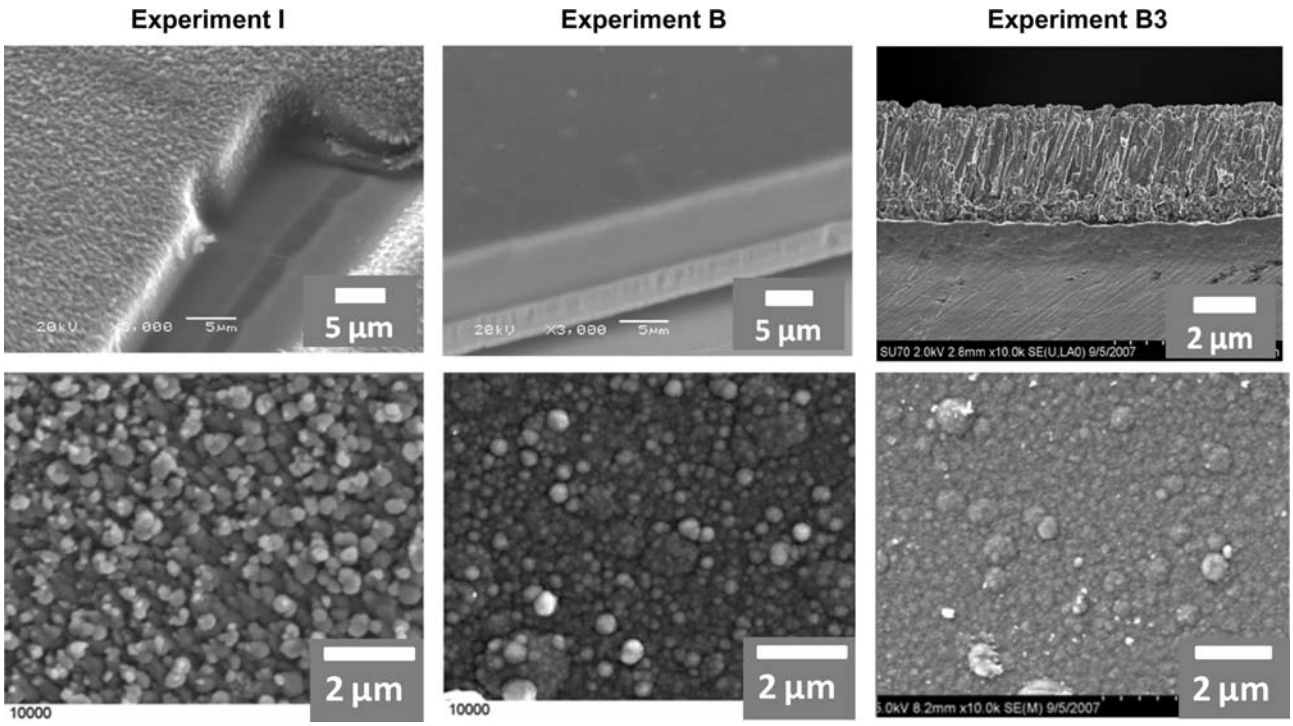

Fig. 4 SEM images: Experiment I (Reference sample), Experiment B (extra N_2 added during Cr and Al sputtering), and Experiment B3 (direct N_2 added during Cr and Al sputtering)

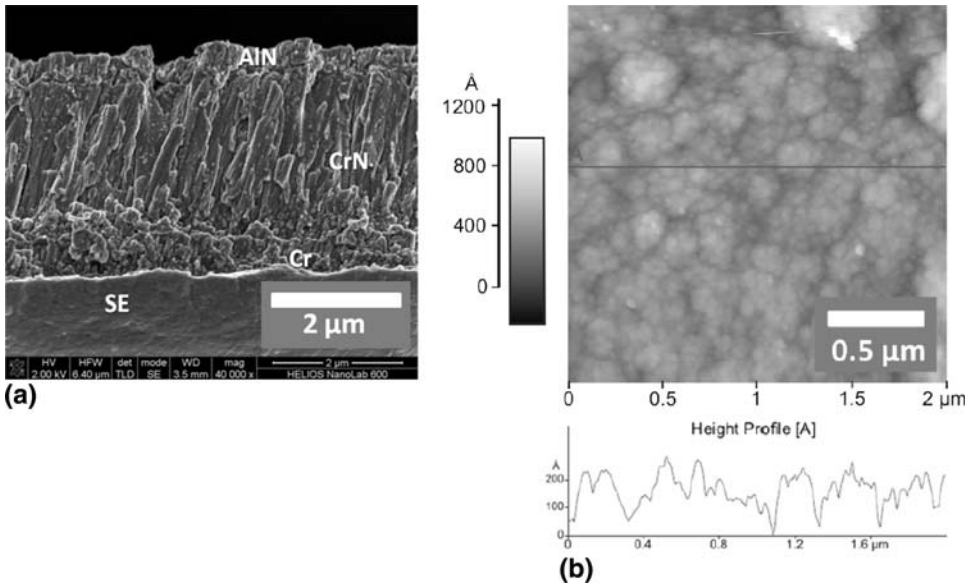

Fig. 5 (a) HRSEM and (b) AFM topography images of sample B3

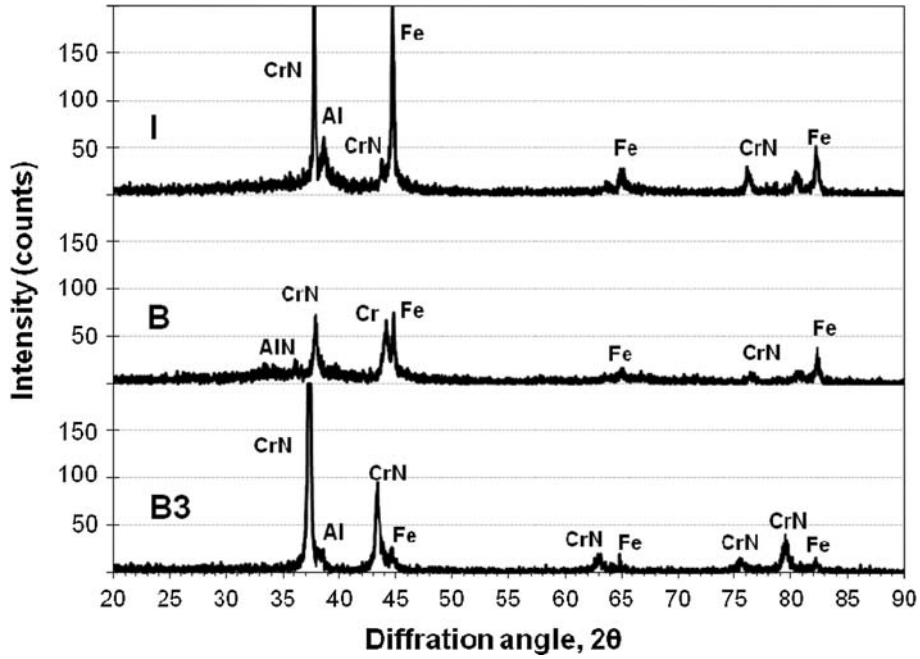

Fig. 6 X-ray diffraction patterns for samples I, B, and B3

effective as increasing the amount of nitrogen in the gas mixture (sample B) for the formation of AlN or the film on this sample was too thin to produce an appreciable XRD signal. In any case, it is clear that in the present conditions, production of CrN occurred much more readily than that of AlN. Since it is clear that the poisoning of the Al target did not occur, the Al sputtered atoms were able to reach the substrate surface, as evidenced by the presence of the pure Al peaks in the XRD results, and that AlN was only clearly observed in sample B; it is likely that the higher concentration of N species in this experiment favored the formation of aluminum nitride while in the base sample, the residence time of the N atoms was too short to complete the seemingly slower reaction for the formation of AlN, and in the case of sample B3, the position of the N_2 flow near the substrate may have resulted in less ionization of the N_2. Thus, further work is required to determine the optimum arrangement for the case of direct N_2 injection to optimize the production of AlN.

3.2 Tribology Results

The objective of the second part of this work was to analyze the surface states of the coated samples in terms of the friction coefficient evolution during dry sliding. The friction tests conducted on the surface of sample B were analyzed and compared to those of an uncoated H13 steel-base sample. The measurements of the coefficient of friction for both samples as a function of sliding distance/laps with a 1 N load

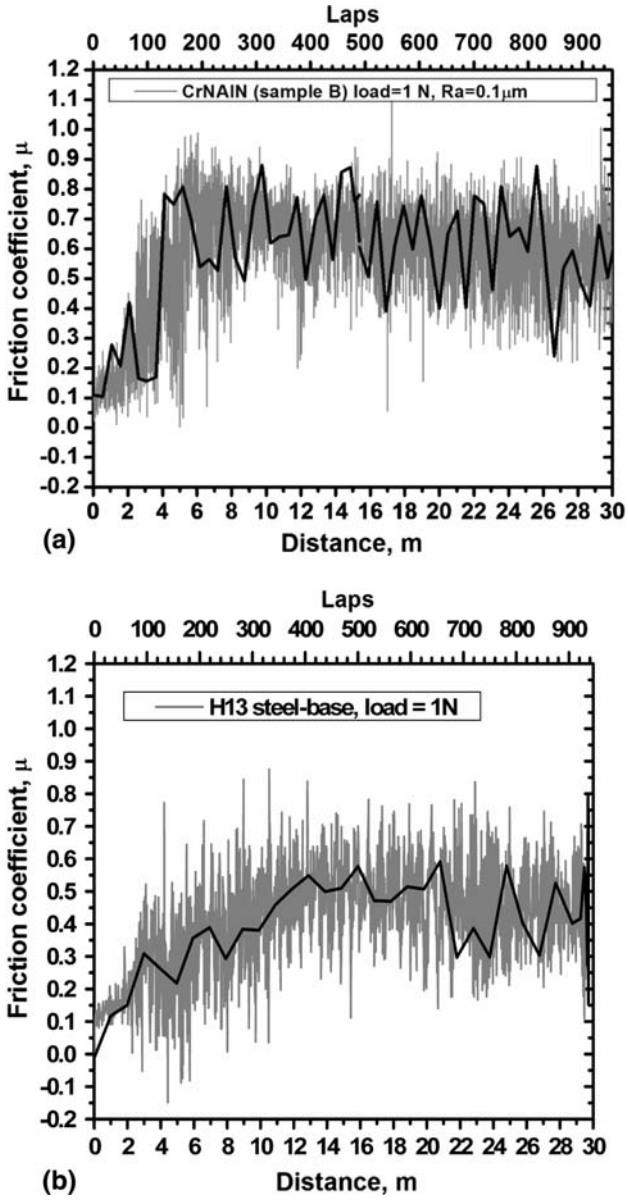

Fig. 7 The variations in coefficient of friction (μ) with the slide distance when hardened-steel pin slid on the surface of (a) CrN/AlN films and (b) H13 steel substrate

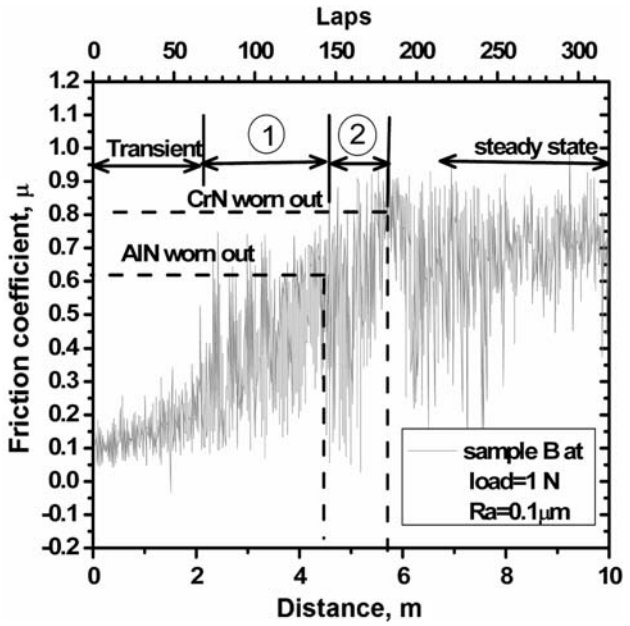

Fig. 8 Sample B showing the worn outs and wear life for each deposited film. This is a magnified view of the running-in period from Fig. 7(a)

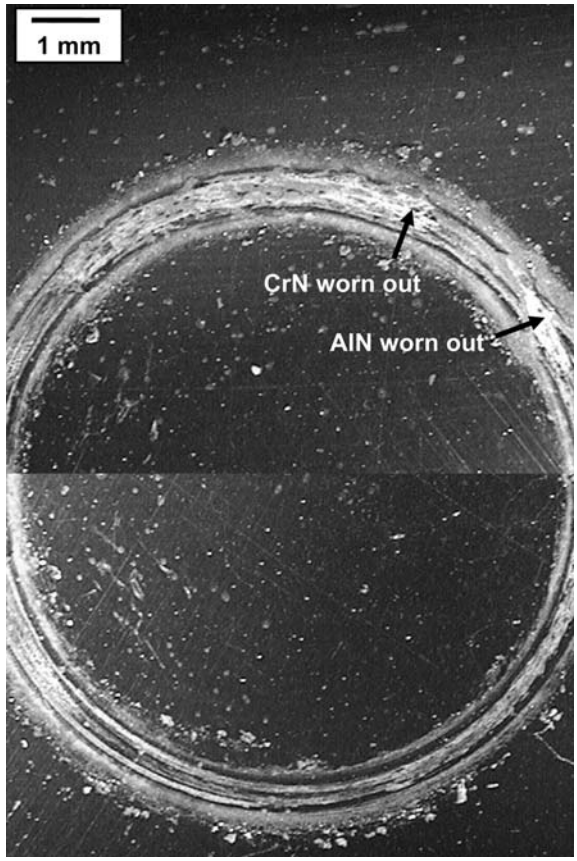

Fig. 9 Wear trace of treated sample B. The *arrows* show the initial location of the failures for each layer

and 14 mm wear track diameter are shown in Fig. 7(a-b). Both curves show the typical running-in period characterized by an initial transient state followed by a friction coefficient increase and a final gradual-steady state. The initial transient state, approximately 2 m sliding distance, corresponds to the contact of the highest asperities of the disk and steel ball surfaces. In this first stage of sliding, the frictional force is largely a result of ploughing of the surface by those asperities. Usually, that initial surface is easily polished until elements of bare surface appear, resulting in a slow increase in the static friction coefficient due to the increased adhesion. After 2 m sliding distance, two fast increments of the friction coefficient for sample B (treated sample of Fig. 7a) were observed. Each jump in the friction coefficient reflects the wearing out of a layer of the deposited film. A greater detail of the running-in period for sample B is depicted in Fig. 8 where it can be seen that the surface layer of AlN exhibited an approximate wear life of 2.5 m sliding distance (≈85 laps), illustrated by the dimension with the circled number one and a friction coefficient of 0.6. The CrN layer, in turn, exhibited an approximate wear life of 1.2 m

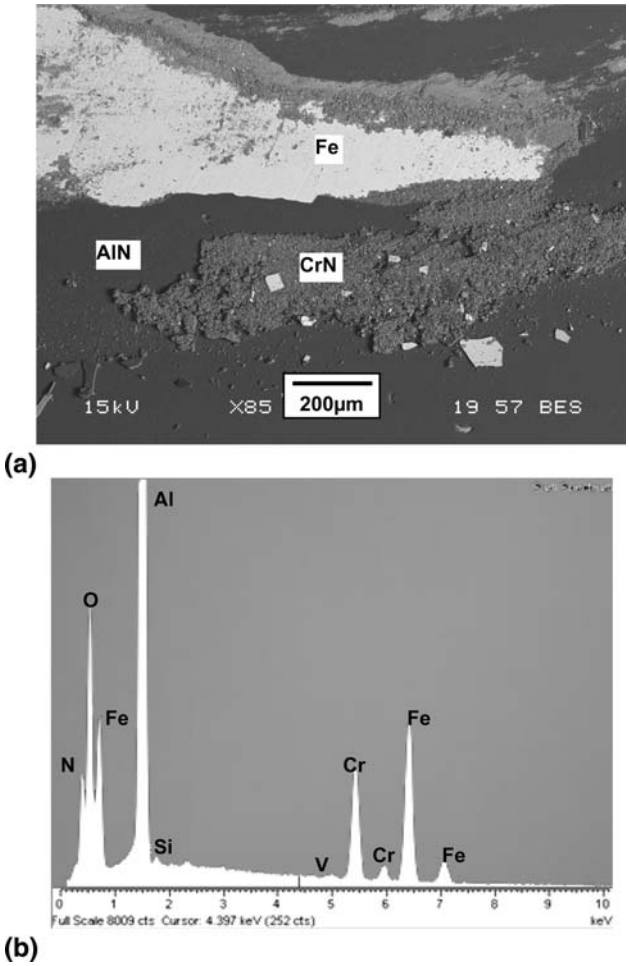

Fig. 10 SEM image + EDS spectral signal. (a) The wear track of treated sample B for 30 m sliding distance. (b) The corresponding EDS spectra revealing the presence of N, Cr, Al, Fe, Si, V, and residual O which can be attributed to oxygen pickup when samples were exposed to air

sliding distance (≈40 laps) as shown by the dimension with the circled number two. As expected, this second layer exhibited an increase in the friction coefficient up to 0.8. The wear pattern on sample B as well as the initial worn out locations for each layer is shown in Fig. 9.

As presented in Fig. 8, the friction behavior is closely related to the structure of the deposited films. The first jump corresponds to the wear out of the AlN layer. Here, the coefficient of friction rises as the number of wear particles rapidly increase, mainly because of the ploughing. At this stage, smooth and rough debris coming from obvious worn grooves-spallation and transferred substances from the ball are present, as can be seen in Fig. 10(a-b). The deformation of asperities continues from the running-in period and the adhesive wear mechanism increases due to larger clean interfacial areas. As mentioned earlier, at a friction coefficient of approximately 0.6, the AlN layer has worn out, i.e. the slider gradually removed the asperities, which graphically is represented by the fall of the friction coefficient (from 4.6 to 5 m sliding distance in Fig. 8) until the first contact between the steel ball and the CrN layer takes place. At this point, the highest asperities make contact and are cut down and crushed by friction contacting stress to form some hard abrasive fine

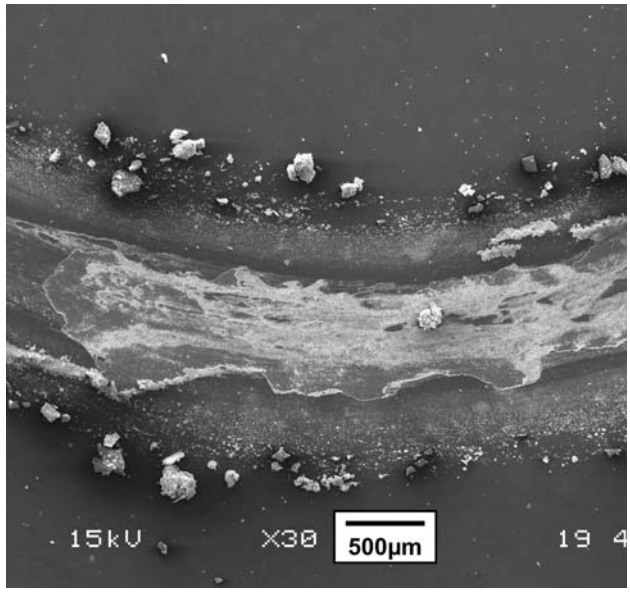

Fig. 11 SEM micrograph of the extended crack of CrN layer of treated sample B worn for 30 m sliding distance

scrapes that adhere to the ball and are pressed into it, resulting in a very fast increase of the friction coefficient. In the course of sliding, the asperities are not only ascribed to the layers but to the transferred little fine particles from the steel ball. This means that the slider is worn and therefore, the contact area is larger so the degree of adhesiveness increases, resulting in higher friction coefficient values and inherently the prompt failure of the layer. The observed load carrying capacity and deformation resistance can be attributed to the thicker layers of CrN than AlN. However, the shorter wear life of the CrN layer may arise from lack of adhesion to the substrate as well as the propagation and extension of cracks as seen in Fig. 11 (Ref 21). In addition, this may also be associated with the development of tensile stresses during deposition.

4. Conclusions

The rate of CrN formation during reactive magnetron sputtering was much faster and easier than that of AlN. Furthermore, the addition of extra nitrogen during reactive magnetron sputtering was more effective for nitride formation than addition between the target and the substrate or directly on the substrate. Tribological properties strongly depended on the composition and thickness of the layers. The CrN layer slightly increased the load-bearing capacity compared to the untreated H13 steel. It is, however, necessary to research the adhesion aspects related to the sputtering processes in order to increase the wear life of this bilayer system.

References

1. K. Holmberg, H. Ronkainen, and A. Matthews, Tribology of Thin Coatings, *Ceram. Int.*, 2000, **26**, p 787–795
2. T. Wierzchon, Structure and Properties of Multicomponent and Composite Layers Produced by Combined Surface Engineering Methods, *Surf. Coat. Technol.*, 2004, **180–181**, p 458–464

3. L. Cunha, M. Andritschky, K. Pischow, and Z. Wang, Microstructure of CrN Coatings Produced by PVD Techniques, *Thin Solid Films*, 1999, **355–356**, p 465–471
4. K.H. Nam, M.J. Jung, and J.G. Han, A Study on the High Rate Deposition of CrNx Films with Controlled Microstructure by Magnetron Sputtering, *Surf. Coat. Technol.*, 2000, **131**, p 222–227
5. M.A. Djouadi, C. Nouveau, O. Banakh, R. Sanjinés, F. Lévy, and G. Nouet, Stress Profiles and Thermal Stability of Cr_xN_y Films Deposited by Magnetron Sputtering, *Surf. Coat. Technol.*, 2002, **151**, p 510–514
6. G. Wei, A. Rar, and J.A. Barbard, Composition, Structure, and Nanomechanical Properties of DC-Sputtered CrN_x ($0 \le x \le 1$) Thin Films, *Thin Solid Films*, 2001, **398–399**, p 460–464
7. P.H. Mayrhofer, G. Tischler, and C. Mitterer, Microstructure and Mechanical/Thermal Properties of Cr-N Coatings Deposited by Reactive Unbalanced Magnetron Sputtering, *Surf. Coat. Technol.*, 2001, **142–144**, p 78–84
8. Z.B. Zhao, Z.U. Rek, S.M. Yalisove, and J.C. Bilello, Phase Formation and Structure of Magnetron Sputtered Chromium Nitride Films: In Situ and Ex-Situ Studies, *Surf. Coat. Technol.*, 2004, **185**, p 329–339
9. J.-W. Lee, S.-K. Tien, Y.-C. Kuo, and C.-M. Chen, The Mechanical Properties Evaluation of the CrN Coatings Deposited by the Pulsed DC Reactive Magnetron Sputtering, *Surf. Coat. Technol.*, 2006, **200**, p 3330–3335
10. Y.B. Gerbig, V. Spassov, A. Savan, and D.G. Chetwynd, Topographical Evolution of Sputtered Chromium Nitride Thin Films, *Thin Solid Films*, 2007, **515**, p 2903–2920
11. S.R. Kirkpatrick, S.L. Rohde, D.M. Mihut, M.L. Kurruppu, J.R. Swanson, D. Thomson, and J.A. Woollam, Process Monitoring and Control of Low Temperature Reactively Sputtered AlN, *Thin Solid Films*, 1998, **332**, p 16–20
12. M. Ishihara, S.J. Li, H. Yumoto, K. Akashi, and Y. Ide, Control of Preferential Orientation of AlN Films Prepared by the Reactive Sputtering Method, *Thin Solid Films*, 1998, **316**, p 152–157
13. B.-H. Hwang, C.-S. Chen, H.-Y. Lu, and T.-C. Hsu, Growth Mechanism of Reactively Sputtered Aluminum Nitride Thin Films, *Mater. Sci. Eng.*, 2002, **A325**, p 380–388
14. Q.X. Guo, M. Yoshitugu, T. Tanaka, M. Nishio, and H. Ogawa, Microscopic Investigations of Aluminum Nitride Thin Films Grown by low-temperature reactive sputtering, *Thin Solid Films*, 2005, **483**, p 16–20
15. K.-H. Chiu, J.-H. Chen, H.-R. Chen, and R.-S. Huang, Deposition and Characterization of Reactive Magnetron Sputtered Aluminum Nitride Thin Films for Film Bulk Acoustic Wave Resonator, *Thin Solid Films*, 2007, **515**, p 4819–4825
16. Accuratus, 2002, http://www.accuratus.com/index.htm. Accessed March 2008
17. S.R. Pulugurtha, D.G. Bhat, M.H. Gordon, and J. Shultz, et al., Mechanical and Tribological Properties of Compositionally Graded CrAlN Films Deposited by AC Reactive Magnetron Sputtering, *Surf. Coat. Technol.*, 2007, **202**, p 1160–1166
18. J. Lin, J.J. Moore, B. Mishra, and M. Pinkas, Effect of Asynchronous Pulsing Parameters on the Structure and Properties of CrAlN Films Deposited by Pulsed Closed Field Unbalanced Magnetron Sputtering (P-CFUBMS), *Surf. Coat. Technol.*, 2008, **202**, p 1418–1436
19. O. Salas, K. Kearns, S. Carrera, and J.J. Moore, Tribological Behavior of Candidate Coatings for Al Die Casting Dies, *Surf. Coat. Technol.*, 2003, **172**, p 117–127
20. "Standard Test Method for Wear Testing with a Pin-on-Disk Apparatus," ASTM G99 95a, 2000
21. D. Landheer and J.H. Zaat, The Mechanism of Metal Transfer in Sliding Friction, *Wear*, 1974, **27**, p 129–145